Bioorganic Chemistry 108 (2021) 104656

Contents lists available at ScienceDirect

Bioorganic Chemistry

journal homepage: www.elsevier.com/locate/bioorg

Multivalent butyrylcholinesterase inhibitor discovered by exploiting dynamic combinatorial chemistry

Shuang Zhao, Jintao Xu, Shixin Zhang, Maochun Han, Yao Wu, Yusi Li, Lei Hu *

School of Pharmacy, Jiangsu University, 301 Xuefu Rd., Zhenjiang, China

ARTICLE INFO

Keywords:
Dynamic combinatorial chemistry
Multivalent interaction
Butyrylcholinesterase
Protein inhibition
Macromolecule

ABSTRACT

In this study, we report the generation of a polymer-based dynamic combinatorial library (DCL) incorporating exchangeable side chains using acylhydrazone formation reaction. In combination with tetrameric butyrylcholinesterase (BChE), the most potent binding side chain was identified, and the information obtained was further used for the synthesis of a multivalent BChE inhibitor. In the *in vitro* biological evaluation, this multivalent inhibitor exhibited not only better inhibitory effect than the commercial reference but also high selectivity on BChE over acetylcholinesterase (AChE).

1. Introduction

Dynamic combinatorial chemistry (DCC) falls into the category of supramolecular chemistry and it utilizes covalent or noncovalent reversible reactions to generate dynamic combinatorial library (DCL) from building blocks with complementary functional groups [1–8]. DCL is fully under thermodynamic control therefore it can respond to the addition of external (*e.g.* enzyme, light, metal ion) or internal (*e.g.* pH, phase change) stimuli due to its adaptive nature, resulting in the formation of more favorable constituents at the cost of other less suitable combinations (Fig. 1). DCL, as a whole, keeps shifting from its initial equilibrium during the interaction with stimuli until an overall optimal state, being the amplification of the best-fit constituent(s), is eventually achieved [9–11]. Among its many applications, DCC has been an outstanding success in chemical biology for identification of novel ligands for diverse protein targets [12–14]. DCC integrates compound library generation and affinity screening in one-pot, offering an efficient strategy for the investigation of ligand–protein interaction as well as subsequent drug development [15–17].

Acetylcholinesterase (AChE) and butyrylcholinesterase (BChE) are two cholinesterase proteins commonly found in mammals [18]. In human body as well as many other mammals, AChE and BChE mainly exist as tetrameric glycoproteins with four identical subunits [19–22]. Different from the well-established physiological property of AChE in regulating cholinergic signaling, the role of BChE has become less elusive only in the recent decade. BChE, also known as pseudocholinesterase, or serum cholinesterase, is a non-specific enzyme that hydrolyzes both acetyl- and butyrylcholine [23,24]. Moreover, while BChE is found in more tissues, such as blood serum, liver and pancreas, than AChE, it exists at much lower concentration in the central and peripheral nervous systems [25]. Nevertheless, previous studies revealed that the level of AChE decreases in patient brain while the level and activity of BChE remain unchanged or even increase during the progression of Alzheimer's disease (AD), suggesting that BChE might play an important role in the late stage of AD [26–28]. Besides, BChE activity has been identified to associate with diabetes, obesity, hydrolysis of hunger hormone Ghrelin and other liver diseases [29–34]. Therefore, developing selective BChE inhibitor is currently becoming more and more an attractive target for multiple therapeutic interests despite the challenges mainly due to its structural similarity to AChE as both enzymes share 65% homologic amino acid sequences [35–37].

Multivalency serves in nature as a fundamental principle for achieving strong interactions [38]. Inspired by multivalency, numerous examples, big as the nest stadium and small as velcro, could be found in our daily life. In biology, multivalent interactions are characterized by the spontaneous, reversible binding of multiple ligands on one biological substrate to multiple receptors on another and play key roles in processes such as adhesion, recognition and signaling [39–42]. One distinct character of multivalent interactions between binding partners is the dramatic gain in affinity, making it a highly efficient tool for the targeted strengthening among different biological entities [43–46]. In the study, a polymer-based DCL was designed and generated through reversible acylhydrazone formation reaction, constructing a dynamic platform with multiple reaction sites (Fig. 2). This polymer-based DCL was further

* Corresponding author.
E-mail address: leihu@ujs.edu.cn (L. Hu).

https://doi.org/10.1016/j.bioorg.2021.104656
Received 7 October 2020; Received in revised form 7 January 2021; Accepted 12 January 2021
Available online 27 January 2021

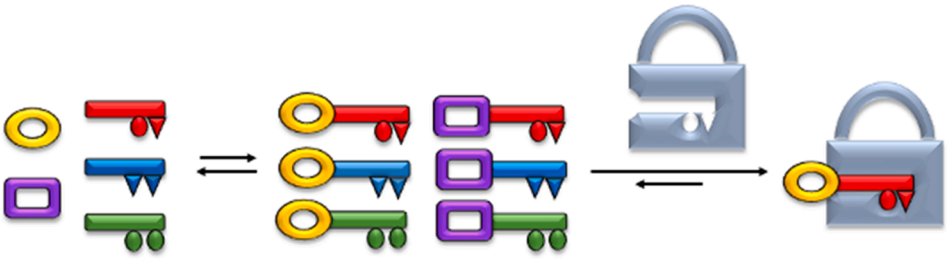

Fig. 1. Conceptual demonstration of DCC.

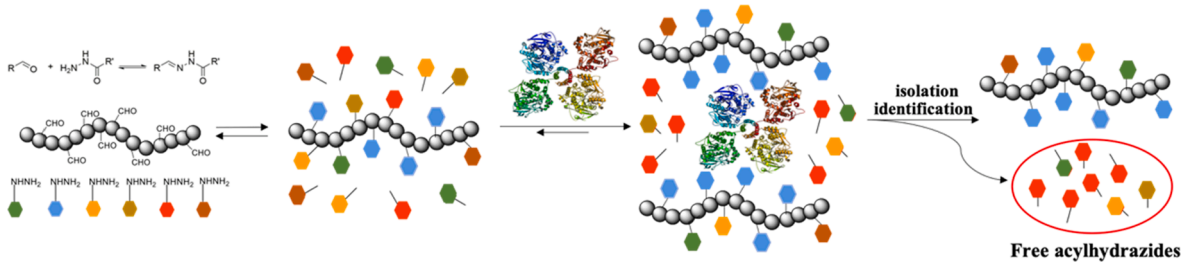

Fig. 2. Schematic illustration of polymer-based multivalent BChE inhibitor identification *via* 'polymer-based' DCC approach.

subjected to the selection of tetrameric BChE through multivalent ligand/receptor interactions. The amplification information obtained from the dynamic system was analyzed and applied for the synthesis of a specific multivalent BChE inhibitor, which proved to be potent and selective comparing to the tested commercial reference.

2. Materials and methods

2.1. Materials

Reagents were used as purchased if not specified. Butyrylcholinesterase (C7512) and acetylcholinesterase (C3389) were purchased from Sigma-Aldrich. ^{1}H NMR and ^{13}C NMR data were recorded on a Bruker Avance 400. Chemical shifts are reported as δ values (ppm), and J values are given in Hertz (Hz). Thin layer chromatography (TLC) was performed on precoated G/UV silica plates (0.20 mm, Qingdao-Haiyang), visualized with UV-detection. Flash column chromatography was performed on silica gel 60, 200–300 mesh (Qingdao-Haiyang). Sephadex G-50 was purchased from Pharmacia Fine Chemicals, Sweden. High-resolution mass spectra were analyzed by Micromon technical corporation, China. Analytical high-performance liquid chromatography (HPLC) with revise phase stationary phases was performed on HP-Agilent 1260 series controller. Solvents for HPLC use were of spectrometric grade. Gel permeation chromatography was performed on a Malvern instrument (Herrenberg, Germany) equipped with a refractive index detector (Viscotek), viscosity detector (Viscotek 270 detector) and Viscotek A-Columns [set 1: A3000 (6 μm, 300 mm × 8 mm) + A2000 (8 μm, 300 mm × 8 mm) and set 2: 2 × A6000M (13 μm, 300 mm × 8 mm)]. Millipore water was used as solvent with 8.5 g/L $NaNO_3$ and 0.2 g/L NaN_3. The flow rate was 0.5 mL/min, and calibration was conducted with poly(ethylene glycol) standards. Absorbance in the IC_{50} evaluation was measured on a Bio-Rad iMark ELISA microtiter plate reader.

2.2. Synthesis

2.2.1. *N-(4-hydroxyphenyl)pyridine-4-carboxamide* ***3e***

4-aminophenol (443 mg, 4.06 mmol), hydroxybenzoic acid (500 mg, 4.06 mmol) and 1-(3-Dimethylaminopropyl)-3-ethylcarbodiimide hydrochloride (934 mg, 4.87 mmol) were dissolved in acetone (25 mL). The mixture was refluxed for 20 h under N_2 atmosphere. The solution was evaporated under vacuum, and the crude product was purified by silica gel chromatography (hexane:EtOAc = 1:1) to yield product **3e** (200 mg, 23%) as a white solid. ^{1}H NMR (400 MHz, DMSO-d_6) δ: 10.29 (s, 1H), 9.36 (s, 1H), 8.77 (d, J = 4.0 Hz, 2H), 7.85 (d, J = 4.0 Hz, 2H), 7.55 (d, J = 8.0 Hz , 2H), 6.78(d, J = 8.0 Hz , 2H). ^{13}C NMR (100 MHz, DMSO-d_6) δ: 163.7, 154.5, 150.6, 142.5, 130.5, 122.8, 121.9, 115.5.

2.2.2. *Ethyl 2-((7-(dimethylamino)naphthalen-2-yl)oxy)acetate* ***4a***

To a solution of 7-*N*,*N*-dimethylamino-2-naphthol (278 mg, 1.48 mmol) and K_2CO_3 (308 mg, 2.22 mmol) in CH_3CN (10 mL) was added ethyl bromoacetate (197 μL, 1.78 mmol) at 0 ℃ dropwise. The reaction mixture was stirred at 0 ℃ for 1 h and then at r.t. overnight, at which time the solution was filtered, and the filtrate was concentrated under vacuum. The crude product was purified by silica gel chromatography (hexane:EtOAc = 8:1) to yield product **4a** (344 mg, 84%) as a white solid. ^{1}H NMR (400 MHz, DMSO-d_6) δ: 7.65–7.61 (m, 2H), 7.06–7.03 (m, 2H), 6.88–6.83 (m, 2H), 4.84 (s, 2H), 4.20 (q, J = 8.0 Hz 2H), 2.98 (s, 6H), 1.23 (t, J = 8.0 Hz, 3H). ^{13}C NMR (100 MHz, DMSO-d_6) δ: 169.2, 156.3, 149.3, 136.2, 129.3, 128.6, 122.3, 114.5, 114.2, 106.1, 105.5, 65.0, 61.0, 40.7, 14.5.

2.2.3. *Ethyl 2-(3-(dimethylamino)phenoxy)acetate* ***4b***

Procedure for compound **4a** was followed. Compound **4b** was obtained as a yellow solid (43%). ^{1}H NMR (400 MHz, $CDCl_3$) δ: 7.14 (t, J = 8.4 Hz, 1H), 6.40 (dd, J = 8.4, 2.0 Hz, 1H), 6.34 (t, J = 2.4 Hz, 1H), 6.23 (dd, J = 7.6, 2.0 Hz, 1H), 4.61 (s, 2H), 4.27 (q, J = 7.2 Hz, 2H), 2.92 (s, 6H), 1.30 (t, J = 7.2 Hz, 3H); ^{13}C NMR (100 MHz, $CDCl_3$) δ: 169.2, 158.9, 152.0, 129.7, 106.6, 101.5, 100.0, 65.5, 61.2, 40.5, 14.2.

2.2.4. *Ethyl 2-(pyridin-3-yloxy)acetate* ***4c***

Procedure for compound **4a** was followed. Compound **4c** was obtained as a white solid (29%). ^{1}H NMR (400 MHz, $CDCl_3$) δ: 8.79 (dd, J = 4.0, 1.6 Hz, 1H), 8.04 (d, J = 8.8 Hz, 2H), 7.46 (dd, J = 9.2, 2.8 Hz, 1H), 7.36 (dd, J = 8.4, 4.4 Hz, 1H), 7.02 (d, J = 2.8 Hz, 1H), 4.75 (s, 2H), 4.30 (q, J = 7.2 Hz, 2H), 1.31(t, J = 6.8 Hz, 3H); ^{13}C NMR (100 MHz, $CDCl_3$) δ: 168.5, 155.9, 148.4, 144.6, 135.0, 131.1, 129.0, 122.1, 121.5, 106.6, 65.6, 61.5, 14.1.

2.2.5. *Ethyl 2-(quinolin-6-yloxy)acetate* ***4d***

Procedure for compound **4a** was followed. Compound **4d** was obtained as a white solid (77%). ^{1}H NMR (400 MHz, $CDCl_3$) δ: 8.34–8.32

(m, 1H), 8.26 (dd, $J = 4.4$, 2.0 Hz, 1H), 7.25–7.18 (m, 2H), 4.57 (s, 2H), 4.26 (q, $J = 7.2$ Hz, 2H), 1.29 (t, $J = 7.2$ Hz, 3H); ^{13}C NMR (100 MHz, $CDCl_3$) δ: 168.2, 154.1, 143.1, 138.0, 123.8, 121.6, 65.5, 61.6, 14.1.

2.2.6. Ethyl 2-(4-(isonicotinamido)phenoxy)acetate **4e**

Procedure for compound **4a** was followed. Compound **4e** was obtained as a white solid. (116 mg, 42%) ^{1}H NMR (400 MHz, DMSO-d_6) δ: 10.41 (s, 1H), 8.78 (d, $J = 5.2$ Hz, 2H), 7.86 (d, $J = 5.2$ Hz, 2H), 7.68 (d, $J = 8.4$ Hz, 2H), 6.96 (d, $J = 8.8$ Hz , 2H), 4.77 (s, 2H), 4.18 (q, $J = 7.2$ Hz, 2H), 1.22 (t, $J = 7.2$ Hz, 3H). ^{13}C NMR (100 MHz, DMSO-d_6) δ: 169.2, 164.0, 154.6, 150.7, 142.4, 132.7, 122.4, 121.9, 115.0, 65.3, 61.0, 14.5.

2.2.7. 7-(2-hydrazinyl-2-oxoethoxy)-N,N,N-trimethylnaphthalen-2-aminium iodide **5a**

To a solution of compound **4a** (324 mg, 1.18 mmol) in CH_3CN was added methyl iodide (1.84 mL, 29.6 mmol). The reaction mixture was stirred at r.t. overnight, at which time the solvent was removed under vacuum. The residue was dissolved in water and filtered. The solvent was removed under vacuum to yield crude methylated product (374 mg). The crude product (20 mg, 0.048 mmol) was dissolved in methanol (3 mL), and hydrazine hydrate (22 μL, o.48 mmol) was added to this solution. The reaction mixture was refluxed for 3 h, at which time the solvent was removed under vacuum. The solid was washed with dichloromethane (10 mL × 3) and dried to yield product **5a** (17 mg, 88%) as a white solid. ^{1}H NMR (400 MHz, D_2O) δ: 8.13 (d, $J = 4.0$ Hz, 1H), 7.99 (d, $J = 8.0$ Hz, 1H), 7.87 (d, $J = 12.0$ Hz, 1H), 7.69–7.66 (m, 1H), 7.31–7.25 (m, 2H), 4.65 (s, 2H), 3.63 (s, 9H). ^{13}C NMR (100 MHz, D_2O) δ: 169.3, 156.4, 144.4, 133.5, 130.6, 129.6, 128.7, 120.7, 117.6, 115.0, 108.1, 65.9, 57.0; HRMS (ESI-TOF): ([M−I], $C_{15}H_{20}N_3O_2$; cal.: 274.1550, found: 274.1549).

2.2.8. 3-(2-hydrazinyl-2-oxoethoxy)-N,N,N-trimethylbenzenaminium iodide **5b**

Procedure for compound **5a** was followed. Compound **5b** was obtained as a yellow solid (55%). ^{1}H NMR (400 MHz, D_2O) δ: 7.58 (t, $J = 8.4$ Hz, 1H), 7.46 (dd, $J = 8.4$, 2.4 Hz, 1H), 7.41 (t, $J = 2.4$ Hz, 1H), 7.17 (dd, $J = 8.0$, 2.0 Hz, 1H), 4.74 (s, 2H), 3.62 (s, 9H); ^{13}C NMR (100 MHz, DMSO-d_6) δ: 166.5, 159.0, 148.6, 131.3, 116.3, 113.2, 108.6, 67.1, 56.9; HRMS (ESI-TOF): ([M−I], $C_{11}H_{18}N_3O_2$; calc.: 224.1394, found: 224.1389).

2.2.9. 6-(2-hydrazinyl-2-oxoethoxy)-1-methylquinolin-1-ium iodide **5c**

Procedure for compound **5a** was followed. Compound **5c** was obtained as a white solid (64%). ^{1}H NMR (400 MHz, D_2O) δ: 9.02 (d, $J = 5.6$ Hz, 1H), 8.95 (d, $J = 8.4$ Hz, 1H), 8.35 (d, $J = 9.6$ Hz, 1H), 7.96–7.91 (m, 2H), 7.66 (d, $J = 2.8$ Hz, 1H), 4.89 (s, 2H), 4.61 (s, 3H); ^{13}C NMR (100 MHz, D_2O) δ: 168.8, 157.3, 147.0, 146.0, 135.05, 131.4, 127.7, 122.1, 120.3, 109.1, 66.4, 45.4; HRMS (ESI-TOF): ([M−I], $C_{12}H_{14}N_3O_2$; calc.: 232.1081, found: 232.7087).

2.2.10. 3-(2-hydrazinyl-2-oxoethoxy)-1-methylpyridin-1-ium iodide **5d**

Procedure for compound **5a** was followed. Compound **5d** was obtained as a red solid (94%). ^{1}H NMR (400 MHz, D_2O) δ: 8.62 (s, 1H), 8.47 (d, $J = 6.0$ Hz, 1H), 8.13 (dd, $J = 9.2$, 2.4 Hz, 1H), 7.917 (dd, $J = 8.8$, 6.0 Hz, 1H), 4.89 (s, 2H), 4.37 (s, 3H); ^{13}C NMR (100 MHz, D_2O) δ: 167.9, 156.5, 138.7, 133.8, 130.7, 128.6, 67.1, 48.5; HRMS (ESI-TOF): ([M−I], $C_8H_{12}N_3O_2$; calc.: 182.0924, found: 182.0918).

2.2.11. 4-((4-(2-hydrazinyl-2-oxoethoxy)phenyl)carbamoyl)-1-methylpyridin-1-ium iodide **5e**

Procedure for compound **5a** was followed. Compound **5e** was obtained as a yellow solid (134 mg, 88%) ^{1}H NMR (400 MHz, DMSO-d_6) δ: 10.82 (s, 1H), 9.36 (s, 1H), 9.20 (d, $J = 8.0$ Hz, 2H), 8.52 (d, $J = 8.0$ Hz, 2H), 7.69 (d, $J = 8.0$ Hz, 2H), 7.01 (d, $J = 8.0$ Hz, 2H), 4.50 (s, 2H), 4.43 (s, 2H), 3.38 (s, 3H). ^{13}C NMR (100 MHz, DMSO-d_6) δ: 167.0, 160.9, 155.3, 148.7, 146.8, 131.9, 126.1, 122.5, 115.3, 66.9, 48.6. HRMS (ESI-TOF): ([M−I], $C_{15}H_{17}N_4O_3$; cal.: 301.12952, found: 301.12944).

Table 1
Characterization of **APG** and **APG5b.**

	Mn[a] (Da)	Mw[b] (Da)	PDI[c]	NMR[d] (Da)
APG	8470	9550	1.128	7684
APG5b	12,000	14,100	1.175	9744

[a] Mn, Number-average molecular weight.
[b] Mw, Weight-average molecular weight.
[c] PDI, Polymer dispersity index is defined as Mw/Mn.
[d] Molecular weight calculated through NMR integration.

2.2.12. N-(4-phenoxyacetohydrazide)pyridine-4-carboxamide **5f**

To a solution of compound **4e** (95 mg, 0.317 mmol) in methanol (3 mL) was added hydrazine hydrate (153 μL, 1.583 mmol). The reaction mixture was refluxed for 3 h, then the solvent was removed under vacuum. The residue was washed with DCM (10 mL × 3) and dried to afford product **5f** (58 mg, 64%) as a white solid. ^{1}H NMR (400 MHz, DMSO-d_6) δ: 10.41 (s, 1H), 9.36 (s, 1H), 8.78 (d, $J = 8.0$ Hz, 2H), 7.86 (d, $J = 4.0$ Hz 2H), 7.68 (d, $J = 8.0$ Hz, 2H), 6.98 (d, $J = 8.0$ Hz , 2H), 4.49 (s, 2H), 4.35 (s, 2H). ^{13}C NMR (100 MHz, DMSO-d_6) δ: 167.1, 164.0, 154.8, 150.7, 142.4, 132.6, 122.4, 121.9, 115.1, 66.9. HRMS (ESI-TOF): ([M+H], $C_{14}H_{15}N_4O_3$; cal.: 287.11387, found: 287.11371).

2.2.13. Acylydrazone polymer APG5b

To a solution of polymer **APG** (50 mg, 0.0065 mmol) in methanol (2 mL) with anhydrous $MgSO_4$ (10 mg) was added compound **5b** (23 mg, 0.065 mmol). The reaction mixture was refluxed for 2 h, then the solution was filtered. The filtrate was concentrated under vacuum, and the crude product was purified by Sephadex G-50 column using water as eluent to yield polymer **APG5b** as a white solid (42 mg, 58%) (characterization see Table 1).

2.3. General procedure of the formation, templating and analysis of DCL

Acylhydrazides (1 μL, 50 mM each dissolved in DMSO), polymer **APG** (1 μL, 50 mM of aldehyde group concentration in 0.1 M, pH 6.2 PBS buffer), aniline (5 μL, 1 M in DMSO) were added to PBS buffer (993 μL, 0.1 M, pH 6.2) in a screw-cap vial, which was assembled onto a rotary mixer at r.t.. 10 h later, pH of the DCL was raised to 8 by addition of aqueous NaOH solution. Polymer was separated by using ultrafiltration (MW cut-off 3500 Da at 10,000 rpm for 10 min). Equilibrium of the DCL was determined by HPLC analysis to verify the free acylhydrazide concentrations.

Butyrylcholinesterase (0.25 eq, 9 mg) was subsequently added to the equilibrated DCL mixture, which was rotated for 20 h at r.t.. pH of the mixture was raised to 8 by addition of aqueous NaOH solution to quench any further exchange, and CH_3CN was added to denature the enzyme. Enzyme and polymer were separated from the reaction mixture by ultrafiltration (MW cut-off 3500 Da at 10,000 rpm for 10 min). The final acylhydrazide distribution was analyzed by HPLC analysis, and the results were compared with that of in equilibrium.

2.4. HPLC condition

Column, a tandem column system with one Agilent Zorbax C8 (3.5 μm, 250 mm × 4.6 mm) and one Agilent InfinityLab Poroshell 120 C18 (4 μm, 250 mm × 4.0 mm) was applied to efficiently separate all constituents; flow rate, 0.5 mL/min; wavelength, 273 nm; injection volume, 20 μL; gradient, NH_4OAc (0.1 M)/MeOH at 85% for 25 min followed by 85–25% over 5 min.

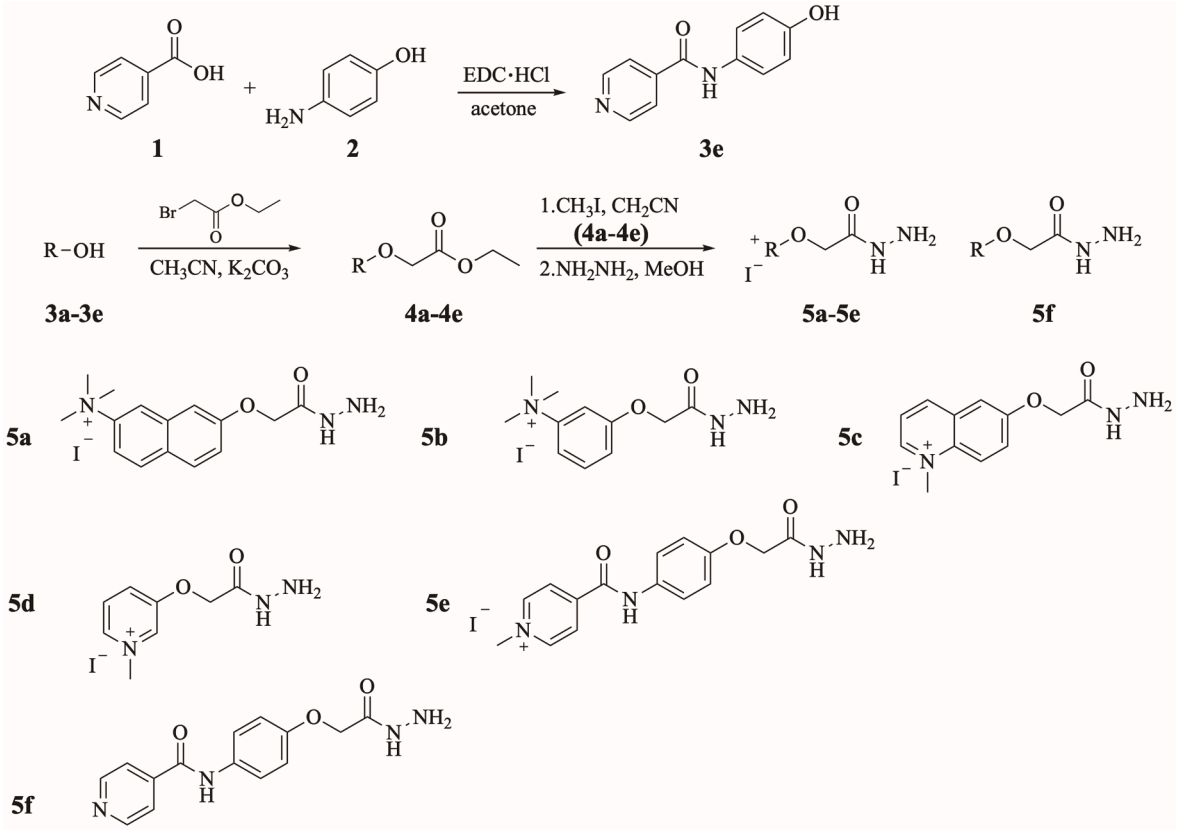

Scheme 1. Synthesis of acylhydrazide derivatives.

2.5. General kinetic studies and determination of K_m

BChE activity assays were carried out by Ellman's method with slight modification [47]. To a solution of 50 mM phosphate buffer (pH 7.4) was added DTNB (250 μM) with different concentration of BTCh to make a total volume of 2 mL. BChE (0.5 U in 1 mL buffer) was added to initiate the hydrolysis process. The formation of 5-thio-2-nitrobenzoate (TNB) was recorded by UV–Vis spectroscopy at 412 nm using a time-drive analysis method over the first 1 min. Blank reactions were performed using buffer solution. K_m was obtained using non-linear regression analysis (GraphPad).

2.6. Determination of inhibition constants

K_i and αK_i were determined using the Ellman method by adding enzyme into BTCh and inhibitor solution. The concentration of BTCh was varied from 10 μM to 240 μM, while the concentration of inhibitor was fixed to 0 nM, 33 nM, 100 nM. Tacrine was used as the reference compound. The inhibition constants were calculated using non-linear regression analysis in a mixed binding model (GraphPad).

2.7. Cytotoxicity evaluation

The cytotoxicity of polymer **APG**, inhibitor **APG5b** and acylhydrazide **5b** against a series of human cancer cell lines was measured using MTT method with slight modification. Doxorubicin was used as reference in this bioassay. Specifically, cells were seeded at a density about 3000 cells/well on a 96-well plate in 100 μL complete medium containing Dulbecco's modified Eagle's medium (DMEM), 5% fetal bovine serum (FBS), 50 unit/mL penicillin and 50 μg/mL streptomycin. After incubation in 5% CO_2 for 12 h at 37 ℃, the medium was removed. Complete medium containing the test material was then added to the well while control experiment without any test sample was conducted at the same time. After an additional 24 h incubation, each well was added with 20 μL of 5 mg/mL MTT stock solution. Then the cells were further incubated for 4 h. Subsequently, staining agent was replaced with 100 μL of DMSO. The plates were placed on a table oscillator for 20 min, and the absorbance was measured at 570 nm. Results were expressed at half maximal inhibitory concentration (IC_{50}), which was the dose of sample leading to a 50% loss of cell viability.

3. Results and discussion

3.1. Design and synthesis of initial binding blocks

Acylhydrazone formation reaction was selected in current study to generate the DCL. This type of reversible reaction has been very often applied to DCC-based medicinal chemistry investigations as acylhydrazone products offer balanced kinetic and thermodynamic properties [48,49]. An aldehyde-functionalized linear poly(glycidol) (**APG**), which was reported in our previous works [11,16] was chosen as the reaction platform. Density of the aldehyde group was optimized to incorporate as many reaction sites while maintaining its water solubility. Accordingly, six acylhydrazides were designed as the complementary binding blocks of polymer **APG** for DCL generation (Scheme 1). Although different in structure, acylhydrazides **5a**-**5e** were all functionalized with quaternary ammonium salt groups, which in principle would specifically interact with certain amino acid residues situated in the active site gorge of BChE through cation-π-binding. A neutral acylhydrazide **5f** was also designed as its close analog was reported to be an effective BChE inhibitor [50]. Specifically, the synthetic route began with the substitution of phenolic compound **3** to ethyl 2-bromoacetate, obtaining intermediate **4**. Compounds **3a**-**3d** were commercially available while compound **3e** was synthesized through amidation between starting materials **1** and **2**. After methylation and hydrazine substitution, intermediates **4a**-**4e** were converted to the corresponding target molecules **5a**-**5e**, and the neutral

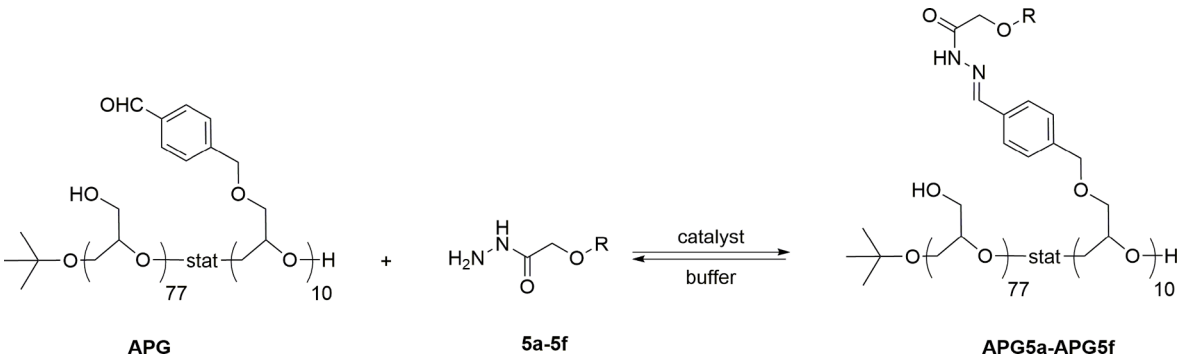

Scheme 2. Generation of dynamic combinatorial library.

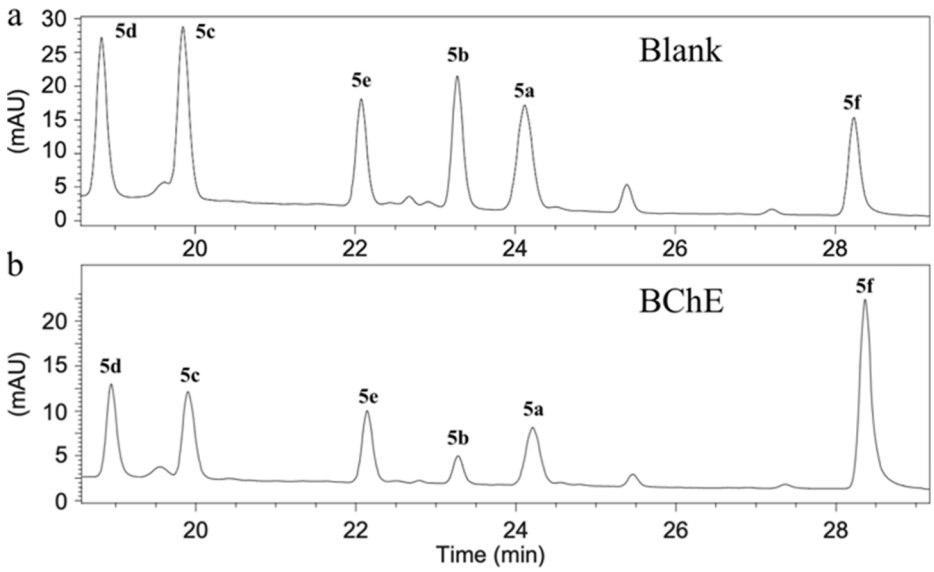

Fig. 3. HPLC chromatographic analyses of free acylhydrazides in DCL: (a) at equilibrium; (b) after BChE intervention.

acylhydrazone **5f** was obtained by skipping the methylation step from intermediate **4e**.

3.2. Generation and equilibrium determination of DCL

Subsequently, the polymer-based DCL was generated by mixing equal molar amount of six acylhydrazone derivatives and aldehyde functionality (0.1 eq. of polymer **APG**) in pH 6.2 PBS buffer using aniline as acylhydrazone formation catalyst (Scheme 2). As concentration of constituents in the DCL was considerably low, NMR spectroscopy was no more a suitable tool for analysis. Instead, HPLC was applied to monitor the process of the dynamic system by analyzing the composition of free acylhydrazides, which were obtained through ultrafiltration, in the reaction mixture. Therefore, distribution of acylhydrazone side chains on the polymer was inversely proportional to that of free acylhydrazines. Under the optimal HPLC conditions, all six acylhydrazides could be detected (Fig. 3a), and the equilibrium was established within 10 h.

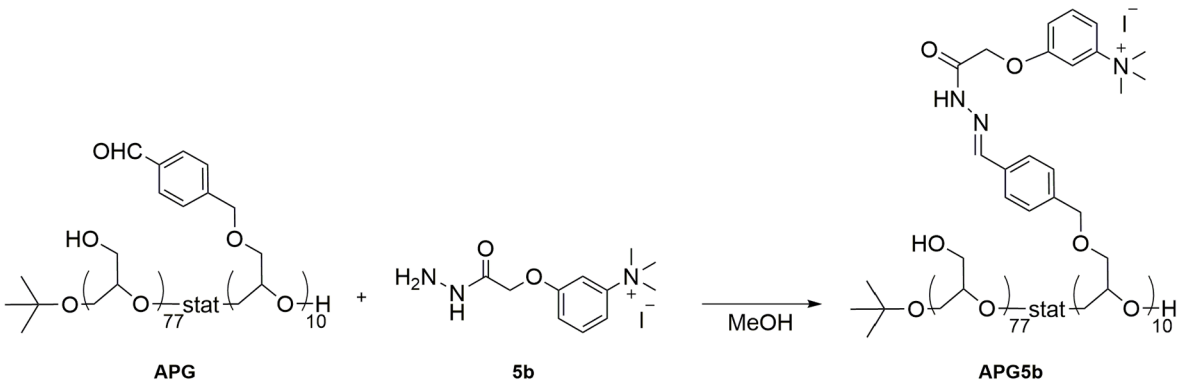

Scheme 3. Synthesis of multivalent BChE inhibitor **APG5b.**

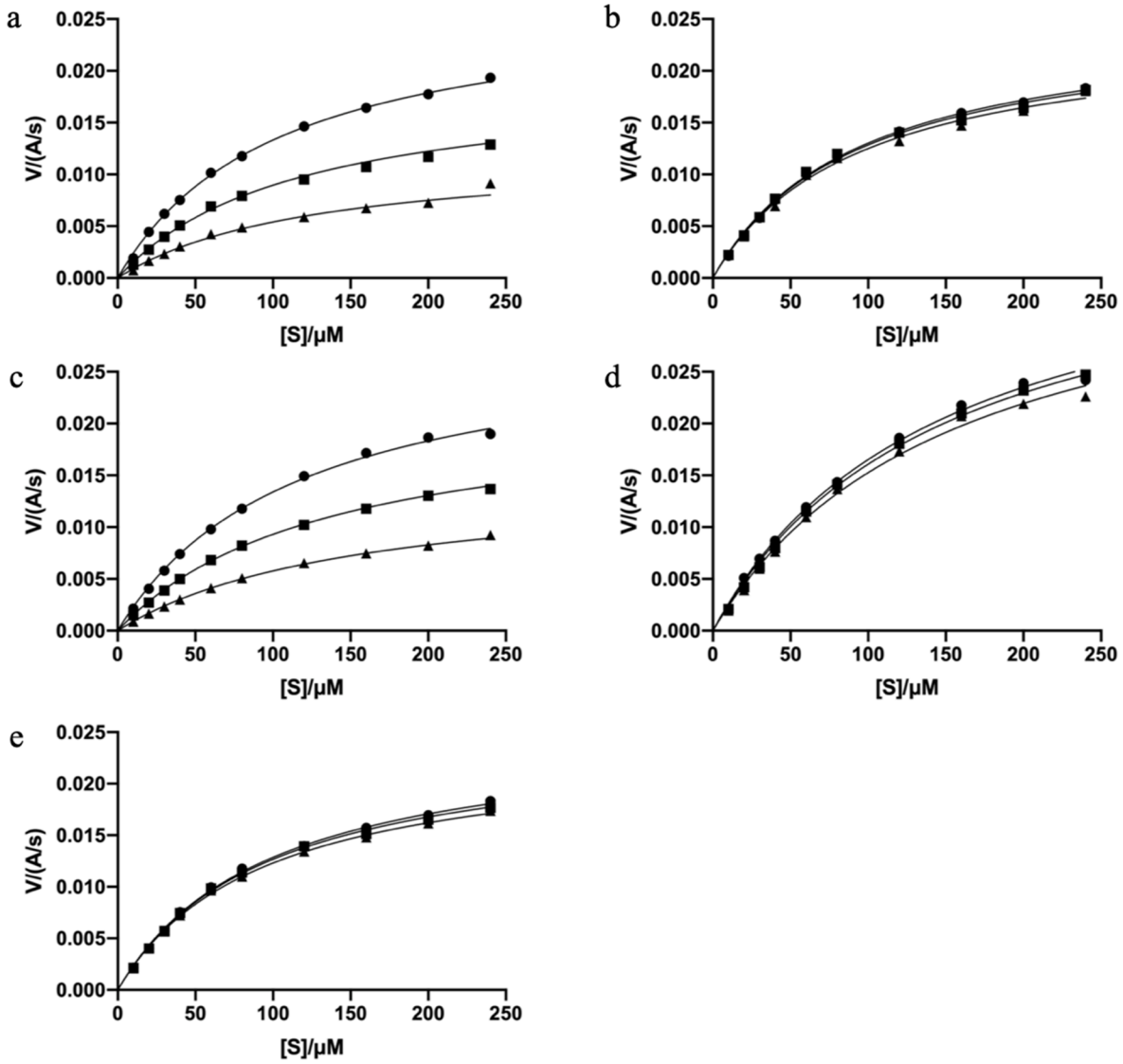

Fig. 4. Inhibition constant of (a) **APG5b** on BChE; (b) monomer **5b** on BChE; (c) Tacrine on BChE; (d) **APG5b** on AChE; (e) monomer **5b** on AChE (●) 0 nM, 33 nM (■), 100 nM (▲).

3.3. Identification of the amplified side chain

With the equilibrium property determined, BChE was added to the equilibrated system. After stirred for 20 h at room temperature, pH of the mixture was adjusted to 8 by addition of NaOH to freeze further exchange, and CH_3CN was added to denature the protein. Free acylhydrazides were separated from the polymer and protein by ultrafiltration. According to the HPLC analysis (Fig. 3b), concentration of acylhydrazide **5b** decreased dramatically, while that of acylhydrazide **5f** sharply increased. The concentration of the rest four hydrazides (**5a**, **5c**, **5e**, **5d**) only decreased slightly compared to acylhydrazide **5b**. The change in free acylhydrazide concentration indicated that acylhydrazide **5b** was preferentially functionalized on the polymer at cost of other less favored constituents through multivalent specific binding to BChE.

3.4. Synthesis of multivalent BChE inhibitor

After identification of amplified constituent, a multivalent BChE inhibitor containing only acylhydrazide **5b** functionalized side chain was synthesized and purified for the following biological evaluation (Scheme 3).

3.5. Measurement of the Michaelis constant and inhibition constant

Slightly modified Ellman's method was applied to determine the Michaelis constant (K_m) of BChE and inhibition constant (K_i) of various substrates. K_m of BChE was determined to be 105 μM, and results indicated that the multivalent inhibitor **APG5b** displayed a mixed inhibition pattern, with a competitive inhibition constant of 59 nM (K_i) and a noncompetitive inhibition constant of 82 nM (αK_i) (Fig. 4a). As a comparison, acylhydrazide **5b** exhibited much lower effective inhibition (Fig. 4b) with K_i = 2.8 μM and αK_i = 2.1 μM. Tacrine, a commercial BChE inhibitor, was used as reference. Compared to **APG5b**, Tacrine showed a very similar inhibition with K_i of 62 nM and αK_i of 102 nM, respectively (Fig. 4c). A possible explanation for the good inhibition potency of polymer **APG5b** was that the polymer and enzyme could form a cross-linked network instead of a 1:1 binding complex, leading to the significant increase in binding affinity. In order to test the selectivity of inhibitor **APG5b**, we also evaluated its inhibitory effect on AChE. Results showed that multivalent inhibitor **APG5b** displayed a K_i of 924 nM and a αK_i of 2.2 μM (Fig. 4d), indicating a good selectivity of inhibitor **APG5b** on BChE over AChE. In addition, K_i of monomer **5b** on AChE was determined to be 5.2 μM (Fig. 4e), which was not significantly different from that of on BChE. However, the inhibition difference of

Table 2
In vitro cytotoxicity evaluation.

	MCF-7 (μM)	A549 (μM)	H1229 (μM)	AC16 (μM)
APG	>256	>256	>256	>256
5b	69.74 ± 2.18	73.29 ± 5.72	99.45 ± 6.42	78.83 ± 5.37
APG5b	182.48 ± 6.57	188.27 ± 5.82	202.19 ± 6.77	179.93 ± 4.28
Doxorubicin	7.92 ± 2.31	10.17 ± 1.84	18.63 ± 2.15	3.56 ± 1.14

monomer **5b** could be further amplified by the multivalent binding capacity of polymer **APG5b**, resulting in the selectivity between enzymes.

3.6. Evaluation of cytotoxicity

Cytotoxicity of multivalent BChE inhibitor **APG5b**, polymer **APG**, acylhydrazide **5b** and reference doxorubicin were evaluated against a series of cell lines, including human breast cancer MCF-7, lung cancer A549 and H1229, human adult cardiomyocyte AC16. As shown in Table 2, polymer **APG** did not display any inhibitory effect against all cell lines, while multivalent inhibitor **APG5b** showed weak cytotoxicity on the tested cell lines. Acylhydrazide **5b** demonstrated moderate cytotoxicity on all cell lines, with IC_{50} values ranging from 69 μM to 99 μM. All results provided possible explanation that the weak cytotoxicity of inhibitor **APG5b** was probably due to the presence of acylhydrazide **5b** functionalized side chains. It was worth noting that the IC_{50} value of multivalent inhibitor **APG5b** was significantly higher than its effective inhibition concentration, indicating that it could be applied as a safe BChE inhibitor.

4. Conclusion

In summary, we have demonstrated the generation of a polymer-based DCL using reversible acylhydrazone formation reaction. In combination with tetrameric BChE, the most active binding side chain was identified and further used for the synthesis of a multivalent inhibitor **APG5b**. In the *in vitro* biological evaluation, this multivalent inhibitor displayed better inhibition on BChE ($K_i = 59$ nM) than Tacrine ($K_i = 62$ nM), and its selectivity between BChE and AChE was also verified. Moreover, *in vitro* cytotoxicity test showed that the synthesized BChE inhibitor was safe for its future applications. The combination of DCC and multivalent interactions in this study was proved to be an efficient strategy for the discovery of novel protein inhibitors and could be applied to the development of other protein targets.

Declaration of Competing Interest

The authors declare that they have no known competing financial interests or personal relationships that could have appeared to influence the work reported in this paper.

Acknowledgments

This work was supported by the Natural Science Foundation of Jiangsu Province (BK20180853), China Postdoc Science Foundation (2019M651717) and the Senior Talent Program of Jiangsu University (17JDG003).

Appendix A. Supplementary material

Supplementary data to this article can be found online at https://doi.org/10.1016/j.bioorg.2021.104656.

References

[1] P. Frei, R. Hevey, B. Ernst, Dynamic combinatorial chemistry: a new methodology comes of age, Chem. – Eur. J. 25 (2019) 60–73.
[2] M. Dumartin, J. Septavaux, M. Donnier-Marechal, E. Jeamet, E. Dumont, F. Perret, L. Vial, J. Leclaire, The dark side of disulfide-based dynamic combinatorial chemistry, Chem. Sci. 11 (2020) 8151–8156.
[3] P.T. Corbett, J. Leclaire, L. Vial, K.R. West, J.L. Wietor, J.K.M. Sanders, S. Otto, Dynamic combinatorial chemistry, Chem. Rev. 106 (2006) 3652–3711.
[4] L. Hu, F. Schaufelberger, B. Timmer, M. Abellán Flos, O. Ramström, Constitutional dynamic chemistry, Kirk-Othmer encyclopedia of chemical technology. Kirk-Othmer Encyclopedia of Chemical Technology, John Wiley & Sons Inc, 2014.
[5] A. Herrmann, Dynamic combinatorial/covalent chemistry: a tool to read, generate and modulate the bioactivity of compounds and compound mixtures, Chem. Soc. Rev. 43 (2014) 1899–1933.
[6] D.A. Fulton, Dynamic combinatorial libraries constructed on polymer scaffolds, Org. Lett. 10 (2008) 3291–3294.
[7] M. Jaegle, E.L. Wong, C. Tauber, E. Nawrotzky, C. Arkona, J. Rademann, Protein-templated fragment ligations—from molecular recognition to drug discovery, Angew. Chem. Int. Ed. 56 (26) (2017) 7358–7378.
[8] R. Huang, I.K.H. Leung, Protein-directed dynamic combinatorial chemistry: a guide to protein ligand and inhibitor discovery, Molecules 21 (7) (2016) 910.
[9] L. Hu, O. Ramström, Silver-catalyzed dynamic systemic resolution of α-iminonitriles in a 1,3-dipolar cycloaddition process, Chem. Commun. 50 (2014) 3792–3794.
[10] A. Wilson, G. Gasparini, S. Matile, Functional systems with orthogonal dynamic covalent bonds, Chem. Soc. Rev. 43 (2014) 1948–1962.
[11] J. Xu, S. Zhang, S. Zhao, L. Hu, Identification and synthesis of an efficient multivalent E. coli heat labile toxin inhibitor — a dynamic combinatorial chemistry approach, Biorg. Med. Chem. 28 (2020), 115436.
[12] C.S. Mahon, M.A. Fascione, C. Sakonsinsiri, T.E. McAllister, W. Bruce Turnbull, D. A. Fulton, Templating carbohydrate-functionalised polymer-scaffolded dynamic combinatorial libraries with lectins, Org. Biomol. Chem. 13 (2015) 2756–2761.
[13] M. Mondal, A.K.H. Hirsch, Dynamic combinatorial chemistry: a tool to facilitate the identification of inhibitors for protein targets, Chem. Soc. Rev. 44 (2015) 2455–2488.
[14] A.M. Hartman, V.R. Jumde, W.A.M. Elgaher, E.M. Te Poele, L. Dijkhuizen, A.K. H. Hirsch, Potential dental biofilm inhibitors: dynamic combinatorial chemistry affords sugar-based molecules that target bacterial glucosyltransferase, ChemMedChem. 15 (2020) 1–12.
[15] A.M. Hartman, W.A.M. Elgaher, N. Hertrich, S.A. Andrei, C. Ottmann, A.K. H. Hirsch, Discovery of small-molecule stabilizers of 14-3-3 protein-protein interactions via dynamic combinatorial chemistry, ACS Med. Chem. Lett. 11 (2020) 1041–1046.
[16] J. Xu, S. Zhao, S. Zhang, J. Pei, Y. Li, Y. Zhang, X. He, L. Hu, Development of a multivalent acetylcholinesterase inhibitor via dynamic combinatorial chemistry, Int. J. Biol. Macromol. 150 (2020) 1184–1191.
[17] R. van der Vlag, H. Guo, U. Hapko, N. Eleftheriadis, L. Monjas, F.J. Dekker, A.K. H. Hirsch, A combinatorial approach for the discovery of drug-like inhibitors of 15-lipoxygenase-1, Eur. J. Med. Chem. 174 (2019) 45–55.
[18] E. Giacobini, Cholinesterases: new roles in brain function and in alzheimer's disease, Neurochem. Res. 28 (2003) 515–522.
[19] A.A. Gorfe, B. Lu, Z. Yu, J.A. McCammon, Enzymatic activity versus structural dynamics: the case of acetylcholinesterase tetramer, Biophys. J. 97 (2009) 897–905.
[20] H.L. Fernandez, R.D. Moreno, N.C. Inestrosa, Tetrameric (G4) acetylcholinesterase: structure, localization, and physiological regulation, J. Neurochem. 66 (1996) 1335–1346.
[21] H. Li, Lawrence M. Schopfer, P. Masson, O. Lockridge, Lamellipodin proline rich peptides associated with native plasma butyrylcholinesterase tetramers, Biochem. J. 411 (2008) 425–432.
[22] Y. Pan, J.L. Muzyka, C.-G. Zhan, Model of human butyrylcholinesterase tetramer by homology modeling and dynamics simulation, J. Phys. Chem. B. 113 (2009) 6543–6552.
[23] K.M. Kutty, R.H. Payne, Serum pseudocholinesterase and very-low-density lipoprotein metabolism, J. Clin. Lab. Anal. 8 (1994) 247–250.
[24] V.P. Whittaker, How the cholinesterases got their modern names, Chem-Biol. Interact. 187 (2010) 23–26.
[25] B. Li, J.A. Stribley, A. Ticu, W. Xie, L.M. Schopfer, P. Hammond, S. Brimijoin, S. H. Hinrichs, O. Lockridge, Abundant tissue butyrylcholinesterase and its possible function in the acetylcholinesterase knockout mouse, J. Neurochem. 75 (2000) 1320–1331.
[26] G. Coban, L. Carlino, A.H. Tarikogullari, S. Parlar, G. Sarıkaya, V. Alptüzün, A. S. Alpan, H.S. Güneş, E. Erciyas, 1H-benzimidazole derivatives as butyrylcholinesterase inhibitors: synthesis and molecular modeling studies, Med. Chem. Res. 25 (2016) 2005–2014.
[27] S. Darvesh, Butyrylcholinesterase as a diagnostic and therapeutic target for alzheimer's disease, Curr. Alzhmer. Res. 13 (2016) 1173–1177.
[28] C. Wu, Y. Tu, Z. Li, Y.F. Li, Highly selective carbamate-based butyrylcholinesterase inhibitors derived from a naturally occurring pyranoisoflavone, Bioorg. Chem. 88 (2019), 102949.
[29] B. Li, J.A. Stribley, A. Ticu, W. Xie, L.M. Schopfer, P. Hammond, S. Brimijoin, S. H. Hinrichs, O. Lockridge, Abundant Tissue butyrylcholinesterase and its possible function in the acetylcholinesterase knockout mouse, J. Neurochem. 75 (3) (2000) 1320–1331.
[30] C.G. Carolan, G.P. Dillon, D. Khan, S.A. Ryder, J.M. Gaynor, S. Reidy, J.F. Marquez, M. Jones, V. Holland, J.F. Gilmer, Isosorbide-2-benzyl Carbamate-5-salicylate, A Peripheral Anionic Site Binding Subnanomolar Selective Butyrylcholinesterase Inhibitor, J. Med. Chem. 53 (2010) 1190–1199.

[31] M. Cucuianu, T. Nistor, N. Hâncu, P. Orbai, C. Muscurel, I. Stoian, Serum cholinesterase activity correlates with serum insulin, C-peptide and free fatty acids levels in patients with type 2 diabetes, Rom. J. Intern. Med. 40 (2002) 43–51.
[32] T. Iwasaki, M. Yoneda, A. Nakajima, Y. Terauchi, Serum butyrylcholinesterase is strongly associated with adiposity, the serum lipid profile and insulin resistance, Intern. Med. 46 (2007) 1633–1639.
[33] B. Li, E.G. Duysen, O. Lockridge, The butyrylcholinesterase knockout mouse is obese on a high-fat diet, Chem-Biol. Interact. 175 (2008) 88–91.
[34] K.K. Sato, T. Hayashi, I. Maeda, H. Koh, N. Harita, S. Uehara, Y. Onishi, K. Oue, Y. Nakamura, G. Endo, H. Kambe, K. Fukuda, Serum butyrylcholinesterase and the risk of future type 2 diabetes: the kansai healthcare study, Clin. Endocrinol. (Oxf.) 80 (2014) 362–367.
[35] Y. Nicolet, O. Lockridge, P. Masson, J.C. Fontecilla-Camps, F. Nachon, Crystal structure of human butyrylcholinesterase and of its complexes with substrate and products, J. Biol. Chem. 278 (2003) 41141–41147.
[36] H. Dvir, I. Silman, M. Harel, T.L. Rosenberry, J.L. Sussman, Acetylcholinesterase: from 3D structure to function, Chem-Biol. Interact. 187 (2010) 10–22.
[37] J. Cheung, M.J. Rudolph, F. Burshteyn, M.S. Cassidy, E.N. Gary, J. Love, M. C. Franklin, J.J. Height, Structures of human acetylcholinesterase in complex with pharmacologically important ligands, J. Med. Chem. 55 (2012) 10282–10286.
[38] C. Fasting, C.A. Schalley, M. Weber, O. Seitz, S. Hecht, B. Koksch, J. Dernedde, C. Graf, E.W. Knapp, R. Haag, Multivalency as a chemical organization and action principle, Angew. Chem. Int. Ed. Engl. 51 (2012) 10472–10498.
[39] M. Huo, Y. Zhao, A.B. Satterlee, Y. Wang, Y. Xu, L. Huang, Tumor-targeted delivery of sunitinib base enhances vaccine therapy for advanced melanoma by remodeling the tumor microenvironment, J. Control. Release. 245 (2017) 81–94.
[40] L. Gao, Q. Li, Z. Deng, B. Brady, N. Xia, Y. Zhou, H. Shi, Highly sensitive protein detection via covalently linked aptamer to MoS(2) and exonuclease-assisted amplification strategy, Int. J. Nanomed 12 (2017) 7847–7853.
[41] O.J. Olatunji, Y. Feng, O.O. Olatunji, J. Tang, Z. Ouyang, Z. Su, D. Wang, X. Yu, Neuroprotective effects of adenosine isolated from Cordyceps cicadae against oxidative and ER stress damages induced by glutamate in PC12 cells, Environ. Toxicol. Pharmacol. 44 (2016) 53–61.
[42] Y.H. Wu, B.Y. Zhang, L.P. Qiu, R.F. Guan, Z.H. Ye, X.P. Yu, Structure properties and mechanisms of action of naturally originated phenolic acids and their derivatives against human viral infections, Curr. Med. Chem. 24 (2017) 4279–4302.
[43] Q. Ouyang, Y. Liu, Q. Chen, Z. Guo, J. Zhao, H. Li, W. Hu, Rapid and specific sensing of tetracycline in food using a novel upconversion aptasensor, Food. Control. 81 (2017) 156–163.
[44] N. Duan, W. Gong, S. Wu, Z. Wang, Selection and application of ssDNA aptamers against clenbuterol hydrochloride based on ssDNA library immobilized SELEX, J. Agric. Food Chem. 65 (2017) 1771–1777.
[45] B. Zhang, H. Li, W. Pan, Q. Chen, Q. Ouyang, J. Zhao, Dual-color upconversion nanoparticles (UCNPs)-based fluorescent immunoassay probes for sensitive sensing foodborne pathogens, Food. Anal. Method. 10 (2017) 2036–2045.
[46] Z. Li, X. Zhou, K. Wang, X. Zhou, J. Shi, X. Huang, H. Mel, A novel sensor for determination of dopamine in meat based on ZnO-decorated reduced graphene oxide composites, Innov. Food Sci. Emerg. Technol. 31 (2015) 196–203.
[47] Y. Zhang, M. Angelin, R. Larsson, A. Albers, A. Simons, O. Ramström, Tandem driven dynamic self-inhibition of acetylcholinesterase, Chem. Commun. (Camb.) 46 (2010) 8457–8459.
[48] C.S. Mahon, A.W. Jackson, B.S. Murray, D.A. Fulton, Templating a polymer-scaffolded dynamic combinatorial library, Chem. Commun. 47 (2011) 7209–7211.
[49] C.S. Mahon, D.A. Fulton, Templation-induced re-equilibration in polymer-scaffolded dynamic combinatorial libraries leads to enhancements in binding affinities, Chem. Sci. 4 (2013) 3661–3666.
[50] X.H. Gao, L.B. Liu, H.R. Liu, J.J. Tang, L. Kang, H. Wu, P. Cui, J. Yan, Structure–activity relationship investigation of benzamide and picolinamide derivatives containing dimethylamine side chain as acetylcholinesterase inhibitors, J. Enzyme Inhib. Med. Chem. 33 (2018) 110–114.